Influence of local-field effects on the radiative lifetime of liquid suspensions of Nd:YAG nanoparticles

Ksenia Dolgaleva and Robert W. Boyd

The Institute of Optics, University of Rochester, Rochester, New York 14627, USA

Peter W. Milonni

104 Sierra Vista Drive, Los Alamos, New Mexico 87544, USA

Received July 24, 2006; revised September 29, 2006; accepted October 13, 2006; posted October 25, 2006 (Doc. ID 73061); published February 15, 2007

We measured the radiative lifetime of Nd:YAG nanopowder with an average particle size of 20 nm suspended in different organic and inorganic liquids. To extract information regarding local-field effects, we fitted the experimental data to three different local-field models: the virtual-cavity (or Lorentz) model, the real-cavity model, and the no-local-field-effects model. The real-cavity model and the no-local-field-effects model can both be adequately fitted to our experimental results, while the virtual-cavity model can be ruled out. © 2007 Optical Society of America

OCIS codes: 160.4760, 160.5690, 160.2540.

It is well known that the rate of spontaneous emission depends in general on the environment of the emitter. The case in which an excited atom is inside a cavity or near a reflecting surface has been studied extensively both theoretically and experimentally.[1] Radiative processes in bulk dielectric media appear to be less well understood at a fundamental level, and in particular there has been much current interest in the effects of local fields on spontaneous emission.[2]

Nanocomposite materials can differ significantly in their optical properties from bulk constituent materials,[3–7] and their growing importance in photonics calls for a better understanding and characterization of the role of local-field and other effects that influence their optical properties. Recent experimental work includes measurements of the radiative lifetimes of Eu^{3+} complexes in liquids,[8] supercritical gases,[9] and glass.[10,11] Here we report the results of measurements of radiative lifetimes of Nd:YAG nanopowders in different liquids. Unlike previous experiments in which the Eu^{3+} is embedded in a ligand cage, surface effects must be considered in the case of nanoparticles of the type used in the present work. However, despite these complications, the experiments described in this paper allow some important conclusions to be drawn about local-field effects. Also, composite materials of the sort studied here may prove useful in the development of photonic devices, and thus an understanding of their optical properties is especially important.

The radiative lifetime is inversely proportional to the Einstein A coefficient, which, in turn, can be expressed through Fermi's golden rule as

$$A = \frac{1}{\tau} = \frac{2\pi}{\hbar}|V_{12}(\omega_0)|^2\rho(\omega_0). \tag{1}$$

Here $V_{12}(\omega_0)$ is the energy of interaction between an emitter and the electric self-field of the emitter in the medium, and $\rho(\omega_0)$ is the density of states at the emission frequency ω_0. In a medium with the average (effective) refractive index n_{eff}, the interaction energy scales as

$$V_{12} \propto \frac{L}{\sqrt{n_{\text{eff}}}}, \tag{2}$$

where L is the local-field correction factor (the ratio of the field acting on an individual emitter to the average field in the medium). The factor L enters the expression for $V_{12}(\omega_0)$ because the microscopic field acting on an individual emitter differs from the macroscopic average field. The factor $\sqrt{n_{\text{eff}}}$ in the denominator of (2) comes from the mode normalization and thus appears in the expression for the electromagnetic energy density in a dielectric medium.[12] The density of states in the medium is proportional to the square of the effective refractive index:

$$\rho(\omega_0) \propto n_{\text{eff}}^2. \tag{3}$$

Using expressions (1)–(3), we can conclude that the spontaneous emission rate A in the medium is related to the spontaneous emission rate A_{vac} in vacuum as

$$A = n_{\text{eff}}L^2A_{\text{vac}}. \tag{4}$$

This relation is easily shown to hold also when the effect of dispersion is included in V_{12} and in the density of states.[12]

Existing theoretical models predict different expressions for the local-field correction factor L. Two models, describing most of the experimental outcomes, are called the virtual-cavity model, or Lorentz model,[13] and the real-cavity model.[14]

To illustrate the virtual-cavity model, let us consider a dielectric medium to be a cubic lattice of point dipoles. One can divide the space around a chosen emitter into a region of nearby dipoles treated as discrete particles and a region of more distant dipoles treated in a continuum approximation. The boundary between the discrete and the uniform regions is a virtual sphere of radius R such that $a \ll R \ll \lambda$, where a is the lattice constant and λ is the wavelength of light. Using the virtual-cavity approach, one arrives at the expression

$$L = \frac{n^2 + 2}{3} \tag{5}$$

for the local-field correction factor.[15,16] Here n is the refractive index of the dielectric medium. The same result for the local-field correction factor can be obtained using a more elegant microscopic approach proposed by Aspnes.[13]

A different expression for the local-field correction factor can be obtained by considering an emitter as being inserted into a tiny cavity inside a dielectric medium.[14] The cavity is assumed to have no material in it except for the emitting dipole under consideration. This theoretical approach is called the real-cavity model. Indeed, in the case in which an emitter replaces some tiny volume of the material, it creates a real cavity inside the dielectric.[2,17] The expression for the local-field correction factor following from the real-cavity model has the form[14]

$$L = \frac{3n^2}{2n^2 + 1}. \tag{6}$$

The expressions (5) and (6) for the local-field correction factor L are very different and lead to different results for the radiative lifetimes in a dielectric medium. In fact, they describe different physical situations.[2,17] The Lorentz model applies to homogeneous dielectric media,[18] while the real-cavity model describes the local-field effects in a medium where the emitters enter in the form of inclusions, or dopants, creating low-polarizability regions in the medium. Examples where the latter model applies are dye molecules dissolved in water droplets suspended in different liquids,[19,20] Eu^{3+} organic complexes suspended in liquids[8] and supercritical gas,[9] liquid suspensions of quantum dots[21] (with the interpretation of the results given in Ref. 17), and Eu^{3+} ions embedded into a binary glass system $x\mathrm{PbO}-(1-x)\mathrm{B_2O_3}$.[10,11]

To the best of our knowledge, there is only one reported experiment on the investigation of local-field effects on the radiative lifetime of liquid suspensions of nanoparticles.[22,23] Based on the theoretical analysis conducted by de Vries and Lagendijk,[2] and on numerous examples of similar experiments,[8,9,19–21] one would expect the radiative lifetime of liquid suspensions of nanoparticles to obey the real-cavity model. Indeed, when placed in a liquid, the nanoparticles create real cavities, replacing some volume of the liquid. It is therefore somewhat surprising that the experimental measurements of the radiative lifetime of Eu^{3+}:Y_2O_3 nanoparticles in liquids, reported in Ref. 22, obeyed the virtual-cavity model. We believe that more experimental studies are needed for a better understanding of local-field effects in liquid suspensions of nanoparticles.

Measurements of the fluorescence lifetime in suspensions of Nd:YAG particles as a function of the refractive index of the surrounding medium were reported in Ref. 24, but not under conditions allowing a study of the influence of local-field effects, which require the particles and the distances between the particles to be much less than the optical wavelength. The observed changes in the fluorescence lifetimes of the Nd:YAG particles were purely the effect of the change in the refractive index on the density of states. The average size of the particles used by the authors of Ref. 24 was of the order of a wavelength of light (several hundreds on nanometers), which made the suspensions of such particles unsuitable for measurements of local-field effects due to the host liquid.

In this paper we present results of measurements of the radiative lifetime of Nd^{3+}:YAG nanoparticles dispersed in different liquids. Our goal is to measure the change in the radiative lifetime of emitters[25] caused by local-field effects and to establish which model for the local-field correction factor works best for our case.

The Nd:YAG nanopowder used in our experiments was manufactured by TAL Materials. According to the scanning electron microscope (SEM) photograph of the nanopowder (see Fig. 1), the average particle diameter was around 20 nm. The Nd concentration was chosen to be 0.9 at. %, which is the standard value for Nd:YAG laser rods. Because of aggregation it was necessary to use appropriate surfactants to obtain good liquid suspensions.

We used 13 different organic and inorganic liquids for suspending the nanoparticles. The liquids and the corresponding values of their refractive indices are shown in Fig. 2. We used the Tween 80 surfactant for water and the aqueous immersion fluid manufactured by Cargille Laboratories, and 12-hydroxystearic acid for oil-based organic liquids (such as carbon tetrachloride and toluene). The aqueous suspensions were sonicated for five minutes, and the resultant dispersions were very stable; the nanoparticles remained in suspension for more than a month. A

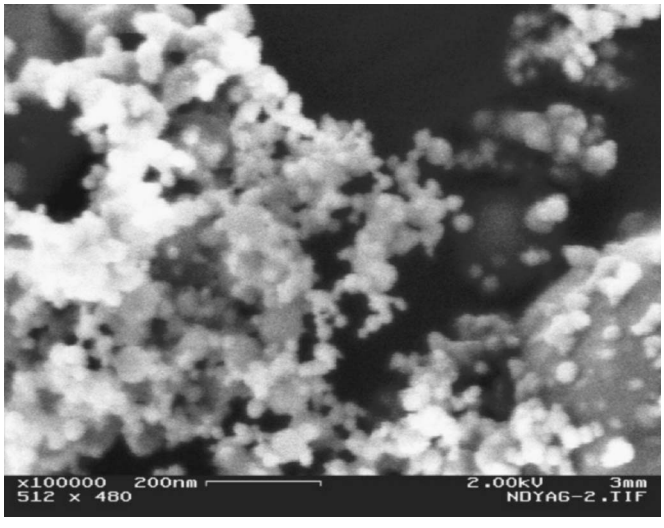

Fig. 1. SEM image of Nd:YAG nanopowder used in our studies.

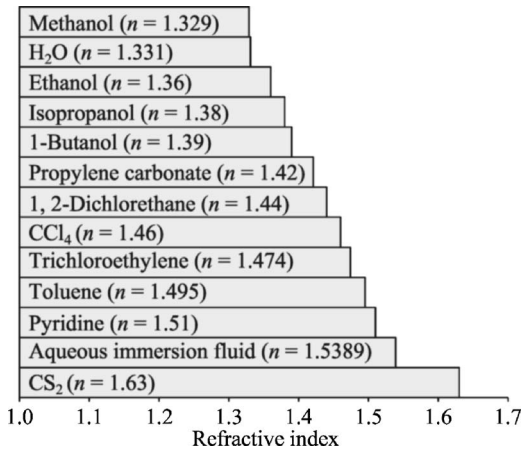

Fig. 2. Liquids used for suspending Nd:YAG nanoparticles with the corresponding refractive indices marked on the horizontal axis.

magnetic stirrer was used to dissolve the surfactants and to suspend the nanoparticles in organic solvents. The most stable organic suspensions were achieved with alcohols, while the oil-based suspensions were only good enough for quick lifetime measurements and sedimented shortly after the measurements were done. The Nd:YAG volume fraction in all the samples was 0.11 vol. %.

As the volume fraction f_{YAG} of the nanoparticles in our samples is very low, we can treat our suspensions as Maxwell-Garnett-type composite materials and use the relation[26,27]

$$\frac{n_{\text{eff}}^2 - n_{\text{liq}}^2}{n_{\text{eff}}^2 + 2n_{\text{liq}}^2} = f_{\text{YAG}} \frac{n_{\text{YAG}}^2 - n_{\text{liq}}^2}{n_{\text{YAG}}^2 + 2n_{\text{liq}}^2} \tag{7}$$

to calculate the effective refractive index n_{eff}. Here n_{liq} is the refractive index of the background liquid, and n_{YAG} is the refractive index of YAG. The effective refractive indices of our samples are very close to the refractive indices of the liquids.

We used a Spectra Physics femtosecond laser system to optically excite Nd ions in the Nd:YAG nanoparticle suspensions. The radiation was generated by a mode-locked Tsunami Ti:sapphire laser, providing 100 fs pulses with 800 nm central wavelength and an initial repetition rate of 80 MHz. The Tsunami laser output was sent to a Spitfire regenerative amplifier, and the repetition rate of the amplifier output was adjusted to 250 Hz, in order to provide enough time between successive pump pulses. The duration of the pulses exiting the regenerative amplifier was around 120 fs, and the pulse energy was close to 1 mJ. The pump radiation was focused into a cell containing the suspension by a lens with a focal length of 100 mm, and the fluorescence from the Nd:YAG nanoparticles was collected by a 50 mm × 50 mm condenser in a perpendicular geometry. A Thorlabs InGaAs detector and a Tectronix digital oscilloscope were used to observe and record the fluorescence decay curves. A narrowband 10 nm FWHM filter with a central wavelength of 1064 nm together with an additional long-pass filter were placed in front of the detector to block scattered pump radiation.

A typical time trace showing the fluorescence decay dynamics is shown in Fig. 3. In all our experiments we observed a nonexponential decay, and our data can be fitted well with the sum of two exponentials with a 4:1 ratio of the slower to the faster decay times. All the slower decay exponentials have fluorescence decay times longer than the typical value 230 μs for bulk Nd:YAG, while all the faster decay exponentials have decay times shorter than that of bulk Nd:YAG. We expect the fluorescence decay times in our Nd:YAG nanopowder suspensions to be longer than that in a bulk Nd:YAG crystal, because the effective refractive indices of our liquid suspensions (1.32–1.63) are smaller than the refractive index of a bulk Nd:YAG (1.82). This is one of the reasons we chose the longer radiative decay time to be compared with different theories describing the local-field effects. Other reasons will be evident from our further analysis.

We performed a series of experiments to determine the origin of the shorter fluorescence decay component. Fluorescence decay dynamics similar to that shown in Fig. 3 was previously observed in a bulk Nd:YAG crystal as a consequence of amplified spontaneous emission.[28] Measuring the fluorescence decay at different pump energies, we did not observe any variations in the two lifetimes and their corresponding amplitudes. We also observed no changes when we varied the geometry of the experiment. All this indicates that the amplified spontaneous emission is not the reason for the biexponential fluorescence decay dynamics in our experiments.

Another possible reason for the faster exponential in the fluorescence decay in our samples could be the contribution from ions sitting on the surfaces of the nanoparticles. To check this hypothesis, we measured the fluorescence lifetimes not only for the Nd:YAG nanopowder, but also for an Nd:YAG micropowder with a micrometer-scale particle size. We obtained the micropowder by crushing a Nd:YAG laser rod and grinding the pieces in a ball mill. The resultant decay dynamics displayed a biexponential character in both powders. The shorter decay time (130 μs) was the same for both powders (within the error of our measurements), and the longer decay time was around 600 μs for the nanopowder and more than two times shorter (270 μs) for the micropowder. Furthermore, the relative contribution of the faster-decay exponential was much higher for the nanopowder, compared with the micropowder. The fact that the shorter lifetime is the

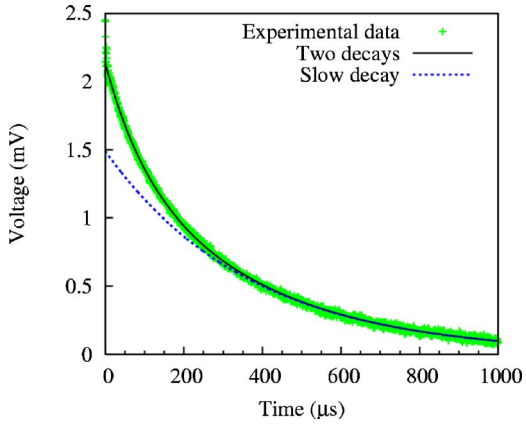

Fig. 3. (Color online) Typical fluorescence decay in the Nd:YAG nanopowder.

same for both powders, and that the faster-exponential amplitude is relatively higher for the nanopowder, suggests that the faster exponential in the fluorescence decay is due to the contribution from the Nd^{3+} ions sitting on the surfaces of the particles. Indeed, the structures of the surfaces of the nanoparticles and microparticles should be similar, while the relative surface area of the nanopowder is much larger than that of the micropowder. The crystal lattice surrounding of the surface ions is distorted, leading to the variations in their electric dipole moments and resulting in much shorter relative decay times. As surface effects are not the topic of our present research, we will concentrate on the analysis of the slower radiative decay component in this paper.

The radiative lifetime of the nanoparticles can be expressed as a function of the effective refractive index of their liquid suspensions by

$$\tau_{\mathrm{rad}} = \frac{\tau_{\mathrm{rad}}^{(\mathrm{vac})}}{n_{\mathrm{eff}}\left(\frac{n_{\mathrm{eff}}^2+2}{3}\right)^2} \tag{8}$$

in the case when the local-field effects obey the Lorentz model and by

$$\tau_{\mathrm{rad}} = \frac{\tau_{\mathrm{rad}}^{(\mathrm{vac})}}{n_{\mathrm{eff}}\left(\frac{3n_{\mathrm{eff}}^2}{2n_{\mathrm{eff}}^2+1}\right)^2} \tag{9}$$

when the local-field effects obey the real-cavity model. Expressions (8) and (9) can be obtained by substituting Eqs. (5) and (6), respectively, into Eq. (4), and taking the inverse of (4) to obtain the fluorescence lifetime. In the absence of local-field effects, the radiative lifetime can be expressed in terms of the effective refractive index of the suspension by the simple relation

$$\tau_{\mathrm{rad}} = \frac{\tau_{\mathrm{rad}}^{(\mathrm{vac})}}{n_{\mathrm{eff}}}. \tag{10}$$

Because we do not know its exact value, we will take the vacuum[29] radiative lifetime $\tau_{\mathrm{rad}}^{(\mathrm{vac})}$ as an adjustable parameter for fitting our experimental data to different models describing the local-field effects.

Generally, the measured decay time is not purely radiative and can be expressed in terms of the radiative and nonradiative decay times as

$$\frac{1}{\tau_{\mathrm{measured}}} = \frac{1}{\tau_{\mathrm{rad}}} + \frac{1}{\tau_{\mathrm{nonrad}}}. \tag{11}$$

It is commonly assumed that the nonradiative decay time A_{nonrad}^{-1} does not depend on the refractive index of the surrounding material[8,20] and can be roughly expressed in terms of the radiative lifetime of ions in vacuum using the relation

$$\eta = \frac{A_{\mathrm{rad}}^{(\mathrm{vac})}}{A_{\mathrm{rad}}^{(\mathrm{vac})} + A_{\mathrm{nonrad}}} \tag{12}$$

for the quantum yield η of the material. Quantum yield is the fraction of the energy decaying through the radiative channel, so the measured lifetime is purely radiative only in the case when the quantum yield of the material is close to unity.

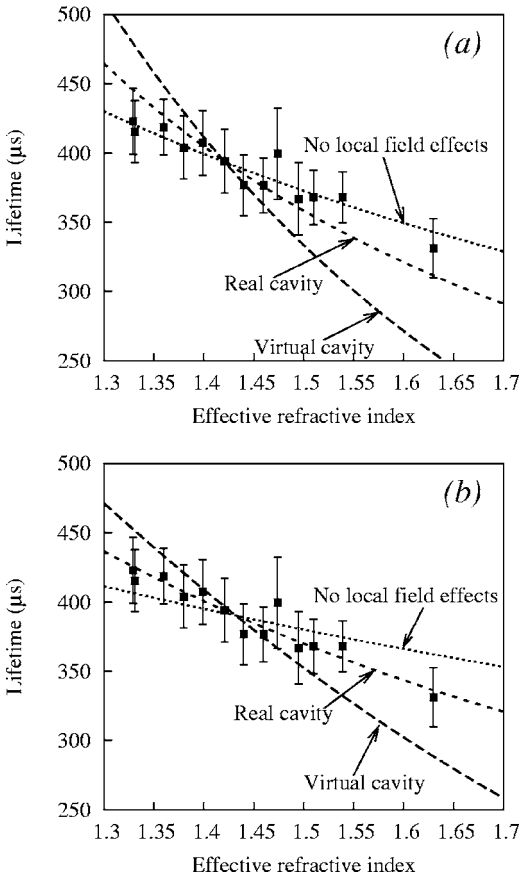

Fig. 4. Experimentally measured radiative lifetimes of the Nd:YAG-nanopowder suspensions (points with error bars), and the best least-squares fits with various models (lines) under the assumption that the quantum yield of the nanopowder is (a) 1 and (b) 0.48.

We were unable to obtain reliable measurements of the absolute quantum yield of our Nd:YAG nanoparticles, in part because of the strong scattering that these particles produce. Instead, we have made use of published values of the quantum yield from bulk samples. Reported values of the quantum yield range from 0.48 (see Ref. 30) to 0.995 (see Ref. 31), with 0.6 being the value most often reported.[32–34] It appears that the quantum yield for a given sample depends sensitively on Nd concentration and on environmental issues. For this reason, we have fitted our data to three different models, given by the Eqs. (8)–(10), for the two limiting values of reported quantum yields, namely 1 and 0.48. Our experimental data together with the best least-squares fit to the data are presented in Fig. 4. The fluorescence lifetimes for the various host liquids (shown as points) are obtained by fitting the time evolution of the fluorescence decay to the sum of two exponentials and taking the longer decay time as the relevant time for the reasons explained above. As the results of the fitting procedure were somewhat sensitive to the range of time values used in the fitting procedure, we repeated the fit for several different time ranges for each data point. The data points shown in Fig. 4 represent av-

erages of the results of these fits, and the error bars represent the standard deviations from the mean values. Figures 4(a) and 4(b) display the results of fitting the experimental data with different local-field models under the assumption of $\eta=1$ and $\eta=0.48$, respectively. Through visual inspection of these results, one can immediately rule out the virtual-cavity model. Under the assumption $\eta=1$, both the real-cavity and the no-local-field-effects models agree reasonably well with the experimental data, with the no-local-field-effects model providing a slightly better fit [see Fig. 4(a)]. However, there is no theoretical justification for assuming the validity of the no-local-field-effects model, as the physical properties of our samples were such that local field effects should have been present. That is, the sizes of the particles were more than 30 times smaller than the wavelength of light. Also the dispersions were stable in most of the samples, which indicates that even if some particle aggregation had occurred, the aggregates were still smaller than the light wavelength. For the other limiting case, with the assumption that $\eta=0.48$ [see Fig. 4(b)], the real-cavity model gives the best fit, which agrees with our expectations based on the theoretical analysis conducted in Ref. 2.

In conclusion, we have investigated the influence of local-field effects on the radiative lifetimes of liquid suspensions of Nd:YAG nanoparticles. To determine which model (the real-cavity, the virtual-cavity model, or no-local-field-effects model) gives the best description of our experimental data, we compared the data with the predictions of these models. We find that the quantitative predictions of these models depend sensitively on the quantum yield of the material samples. Under our experimental conditions, it was not possible to make accurate measurements of this quantity. Instead, we analyzed our data using the range of quantum yields reported in the literature for bulk Nd:YAG. We find that we can rule out the virtual-cavity model as it is in obvious disagreement with our data for any of the values of the quantum yield that we considered. We also find that the real-cavity model can be used to provide a good fit to our data for the range of possible quantum yields. However, we cannot rule out the no-local-fields model on experimental grounds. If we assume that quantum yield is unity, the no-local-fields model is also in good agreement with our data. However, there is no theoretical reason to believe that local field effects would not occur in these materials, and for this reason we believe that the real-cavity model best describes our experimental results.

ACKNOWLEDGMENTS

We gratefully thank C. R. Stroud, J. P. Dowling, and J. E. Sipe for valuable discussions related to the studies. The portion of this work conducted at the University of Rochester was supported by the Airborne Reconaissance Office through a Multidisciplinary University Research Initiative grant and by the National Science Foundation.

REFERENCES AND NOTES

1. P. R. Berman, ed., *Cavity Quantum Electrodynamics* (Academic, 1994).
2. P. de Vries and A. Lagendijk, "Resonant scattering and spontaneous emission in dielectrics: microscopic derivation of local-field effects," Phys. Rev. Lett. **81**, 1381–1384 (1998).
3. J. E. Sipe and R. W. Boyd, "Nonlinear susceptibility of composite optical materials in the Maxwell Garnett model," Phys. Rev. A **46**, 1614–1629 (1992).
4. R. J. Gehr and R. W. Boyd, "Optical properties of nanostructured optical materials," Chem. Mater. **1996**, 1807–1819.
5. E. Snoeks, A. Lagendijk, and A. Polman, "Measuring and modifying the spontaneous emission rate of erbium near an interface," Phys. Rev. Lett. **74**, 2459–2462 (1995).
6. G. L. Fischer, R. W. Boyd, R. J. Gehr, S. A. Jenekhe, J. A. Osaheni, J. E. Sipe, and L. A. Weller-Brophy, "Enhanced nonlinear optical response of composite materials," Phys. Rev. Lett. **74**, 1871–1874 (1995).
7. V. M. Shalaev and M. I. Stockman, "Fractals: optical susceptibility and giant Raman scattering," Z. Phys. D: At., Mol. Clusters **10**, 71–79 (1988).
8. G. L. J. A. Rikken and Y. A. R. R. Kessener, "Local field effects and electric and magnetic dipole transitions in dielectrics," Phys. Rev. Lett. **74**, 880–883 (1995).
9. F. J. P. Schuurmans, D. T. N. de Lang, G. H. Wegdam, R. Sprik, and A. Lagendijk, "Local-field effects on spontaneous emission in a dense supercritical gas," Phys. Rev. Lett. **80**, 5077–5080 (1998).
10. G. M. Kumar, D. N. Rao, and G. S. Agarwal, "Measurement of local field effects of the host on the lifetimes of embedded emitters," Phys. Rev. Lett. **91**, 203903 (2003).
11. G. M. Kumar, D. N. Rao, and G. S. Agarwal, "Experimental studies of spontaneous emission from dopants in an absorbing dielectric," Opt. Lett. **30**, 732–734 (2005).
12. P. W. Milonni, "Field quantization and radiative processes in dispersive dielectric media," J. Mod. Opt. **42**, 1991–2004 (1995).
13. D. E. Aspnes, "Local-field effects and effective-medium theory: a microscopic perspective," Am. J. Phys. **50**, 704–709 (1982).
14. R. J. Glauber and M. Lewenstein, "Quantum optics of dielectric media," Phys. Rev. A **43**, 467–491 (1991).
15. H. A. Lorentz, *Theory of Electrons*, 2nd ed. (Teubner, 1916).
16. J. D. Jackson, *Classical Electrodynamics* (Wiley, 1962).
17. C.-K. Duan, M. F. Reid, and Z. Wang, "Local field effects on the radiative lifetime of emitters in surrounding media: virtual- or real-cavity model?" Phys. Lett. A **343**, 474–480 (2005).
18. J. J. Maki, M. S. Malcuit, J. E. Sipe, and R. W. Boyd, "Linear and nonlinear optical measurements of the Lorentz local field," Phys. Rev. Lett. **67**, 972–975 (1991).
19. P. Lavallard, M. Rosenbauer, and T. Gacoin, "Influence of surrounding dielectrics on the spontaneous emission of sulforhodamine B molecules," Phys. Rev. A **54**, 5450–5453 (1996).
20. G. Lamouche, P. Lavallard, and T. Gacoin, "Optical properties of dye molecules as a function of the surrounding dielectric medium," Phys. Rev. A **59**, 4668–4674 (1999).
21. S. F. Wuister, C. de Mello Donega, and A. Meijerink, "Local-field effects on the spontaneous emission rate of CdTe and CdSe quantum dots in dielectric media," J. Chem. Phys. **121**, 4310–4315 (2004).
22. R. S. Meltzer, S. P. Feofilov, B. Tissue, and H. B. Yuan, "Dependence of fluorescence lifetimes of Y_2O_3:Eu^{3+} nanoparticles on the surrounding medium," Phys. Rev. B **60**, R14012–R14015 (1999).
23. The composites containing Eu^{3+} embedded in a ligand cage (Refs. 8 and 9) are fundamentally different from the sort of nanocomposite material considered in Ref. 22 and in the present work.
24. H. P. Christensen, D. R. Gabbe, and H. P. Jenssen, "Fluorescence lifetimes for neodymium-doped yttrium aluminum garnet and yttrium oxide powders," Phys. Rev. B **25**, 1467–1473 (1982).
25. In this paper we consider the Nd^{3+}:YAG nanoparticles to be the emitters in our composite materials.

26. J. C. Maxwell Garnett, "Colours in metal glasses and in metallic films," Philos. Trans. R. Soc. London Ser. A **203**, 384–420 (1904).
27. J. C. Maxwell Garnett, "Colours in metal glasses in metallic films and in metallic solutions," Philos. Trans. R. Soc. London, Ser. A **205**, 237–288 (1906).
28. N. P. Barnes and B. M. Walsh, "Amplified spontaneous emission: application to Nd:YAG lasers," IEEE J. Quantum Electron. **35**, 101–109 (1999).
29. By "vacuum" we mean the radiative lifetime of an ion placed in the same chemical environment but for a medium of refractive index of unity.
30. T. S. Lomheim and L. G. DeShazer, "Determination of optical cross sections by the measurement of saturation flux using laser-pumped laser oscillators," J. Opt. Soc. Am. **68**, 1575–1579 (1978).
31. T. Kushida and J. E. Geusic, "Optical refrigeration in Nd-doped yttrium aluminum garnet," Phys. Rev. Lett. **21**, 1172–1175 (1968).
32. S. Singh, R. G. Smith, and L. G. Van Uitert, "Stimulated-emission cross section and fluorescent quantum efficiency of Nd^{3+} in yttrium aluminum garnet at room temperature," Phys. Rev. B **10**, 2566–2572 (1974).
33. A. Rosencwaig and E. A. Hildum, "Nd^{3+} fluorescence quantum-efficiency measurements with photo acoustics," Phys. Rev. B **23**, 3301–3307 (1981).
34. C. J. Kennedy and J. D. Barry, "New evidence on quantum efficiency of Nd:YAG," Appl. Phys. Lett. **31**, 91–92 (1977).